Investigating the Impact of Dimer Interface Mutations on Norrin's Secretion and Norrin/β-Catenin Pathway Activation

Min Liu,[1,3] Erkuan Dai,[2] Mu Yang,[1,3] Shujin Li,[1,3] Lin Fan,[4] Yining Liu,[1,3] Haodong Xiao,[2] Peiquan Zhao,[2] and Zhenglin Yang[1,3,4]

[1]Sichuan Provincial Key Laboratory for Human Disease Gene Study, Center for Medical Genetics and Department of Laboratory Medicine, Sichuan Provincial People's Hospital, University of Electronic Science and Technology of China, Chengdu, China
[2]Department of Ophthalmology, Xin Hua Hospital Affiliated to Shanghai Jiao Tong University School of Medicine, Shanghai, China
[3]Research Unit for Blindness Prevention, Chinese Academy of Medical Sciences (2019RU026), Sichuan Provincial People's Hospital, Chengdu, Sichuan, China
[4]The University of Chinese Academy of Sciences, Beijing, China

Correspondence: Zhenglin Yang, Sichuan Provincial People's Hospital, Chengdu, Sichuan 610072, China; yangzhenglin@cashq.ac.cn.
Peiquan Zhao, Department of Ophthalmology, Xin Hua Hospital Affiliated to Shanghai Jiao Tong University School of Medicine, Shanghai 200092 China; zhaopeiquan@126.com.
Erkuan Dai, Department of Ophthalmology, Xin Hua Hospital Affiliated to Shanghai Jiao Tong University School of Medicine, Shanghai 200092 China; daierkuan@126.com.

ML and ED contributed equally to this work.

PURPOSE. This study aimed to investigate the impact of 21 *NDP* mutations located at the dimer interface, focusing on their potential effects on protein assembly, secretion efficiency, and activation of the Norrin/β-catenin signaling pathway.

METHODS. The expression level, secretion efficiency, and protein assembly of mutations were analyzed using Western blot. The Norrin/β-catenin signaling pathway activation ability after overexpression of mutants or supernatant incubation of mutant proteins was tested in HEK293STF cells. The mutant norrin and wild-type (WT) FZD4 were overexpressed in HeLa cells to observe their co-localization. Immunofluorescence staining was conducted in HeLa cells to analyze the subcellular localization of Norrin and the Retention Using Selective Hook (RUSH) assay was used to dynamically observe the secretion process of WT and mutant Norrin.

RESULTS. Four mutants (A63S, E66K, H68P, and L103Q) exhibited no significant differences from WT in all evaluations. The other 17 mutants presented abnormalities, including inadequate protein assembly, reduced secretion, inability to bind to FZD4 on the cell membrane, and decreased capacity to activate Norrin/β-catenin signaling pathway. The RUSH assay revealed the delay in endoplasmic reticulum (ER) exit and impairment of Golgi transport.

CONCLUSIONS. Mutations at the Norrin dimer interface may lead to abnormal protein assembly, inability to bind to FZD4, and decreased secretion, thus contributing to compromised Norrin/β-catenin signaling. Our results shed light on the pathogenic mechanisms behind a significant proportion of NDP gene mutations in familial exudative vitreoretinopathy (FEVR) or Norrie disease.

Keywords: norrin mutations, dimer interface, familial exudative vitreoretinopathy (FEVR), secretion efficiency, norrin/β-catenin signaling pathway

Familial exudative vitreoretinopathy (FEVR) is an inherited retinopathy characterized by abnormal development of retinal blood vessels, leading to manifestations such as retinal hypo vascularization, neovascularization, retinal detachment, and vision loss.[1] Currently, the following 17 genes and one locus have been reported to be associated with FEVR: *ATOH7*,[2] *EVR3* on chromosome 11p12-13,[3] *ILK*,[4] *LRP5*,[5] *LRP6*,[6] *FZD4*,[7] *TSPAN12*,[8] *NDP*,[9] *ZNF408*,[10] *KIF11*,[11] *CTNNA1*,[12] *CTNNB1*,[13] *JAG1*,[14] *DLG1*,[15] *TGFBR2*,[15] *CTNND1*,[16] *SNX31*,[17] and *EMC1*.[18] A significant proportion of reported pathogenic genes are concentrated in genes related to the Wnt pathway, with *NDP*, *FZD4*, *LRP5*, and *TSPAN12* being the 4 most commonly implicated genes.

Norrin, a cysteine-rich secreted growth factor encoded by the Norrin protein (*NDP*) gene, plays a crucial role in retinal angiogenesis, neuroprotection, and the maintenance of blood-retina and blood-brain barriers.[19] Mutations in the *NDP* gene have been identified as being associated with various pediatric vitreoretinopathies, including FEVR, Norrie disease (ND) and retinopathy of prematurity (ROP).[20,21] The primary function of Norrin is to activate the Norrin/β-catenin signaling pathway by binding to the FZD4 receptor, the co-receptor LRP5 or LRP6, and the co-activator TSPAN12.[8,22]

From a structural point of view, Norrin binds to a pair of FZD4 proteins in the form of a homodimer stabilized by 3 pairs of intermolecular disulfide bonds, extensive hydrogen bonds, and hydrophobic interactions.[23] In mice lacking Norrin, delayed development of the superficial vascular plexus and a complete absence of intraretinal capillaries have been observed.[24]

A recent study conducted a comprehensive review of published literature on *NDP* mutations, identifying a total of 201 unique mutations, with 85 of them being missense mutations.[20] Only a small fraction of these single amino acid mutations has been assessed for their potential to activate Norrin/β-catenin pathway activation, and there is limited research on their specific functional alterations. Further, whereas dimerization is considered to be a critical property of Norrin,[19] its significance and the functional consequences of mutations at the dimerization interface of Norrin remain unclear. Additionally, Norrin's secretion mechanism and whether mutations affect its secretion are yet to be fully understood. To address these gaps in the literature, we investigated the pathogenesis of 21 Norrin mutations located at the dimerization interface. We found that proper protein assembly plays a crucial role in Norrin secretion, FZD4 binding, and Norrin/β-catenin signaling pathway activation.

MATERIALS AND METHODS

Cell Culture and Plasmids Construction

HEK293T cells, HEK293STF cells, and HeLa cells (American Type Culture Collection and Cell Systems) were cultured in Dulbecco's Modified Eagle's Medium supplemented with 10% fetal bovine serum a 1% (vol/vol) penicillin/streptomycin at 37°C in a humidified, 5% CO_2 incubator.

The human *NDP* (NM_000266) coding sequence was subcloned into the pCMV6 vector with different tags. Refer to Supplementary Table S1 for the amino acid sequences of the C-terminal tags. The Retention Using Selective Hook (RUSH) construct was generated by substituting VSVG-SBP-EGFP by NDP-SBP-EYFP in the Str-Ii_VSVG-SBP-EGFP (65300, Addgene). The mutations were introduced into the corresponding WT expression plasmid by site-directed mutagenesis with the Q5 Site-Directed Mutagenesis Kit (New England Biolabs). The FZD4 plasmid, FZD5 plasmid, LRP5 plasmid, and pDsRed2-endoplasmic reticulum (ER) plasmid were obtained from Youbio Biotechnology. Either the HA or ECFP tag was fused into the C-terminal of the FZD4 and FZD5 plasmid. The pGL4.1-Renilla was sourced from Promega. Plasmids were transfected by EntransterTM-H4000 transfection reagent (Engreen Biosystem).

Western Blot and Co-Immunoprecipitation

HEK293T cells and HeLa cells were seeded into 24-well plates and transfected with 400 ng NDP-Myc-FLAG or mutant plasmids. The culture medium was replaced with the Wayne293 transfection medium (QuaCell Biotechnology) 6 hours later. After 48 hours, the culture medium was collected. Total cell protein was extracted on ice with lysis buffer (150 mM NaCl, 50 mM Tris-HCl pH 8.0, and 1% Triton X-100) in the presence of protease inhibitor cocktail (MCE). Cell lysates and culture medium were mixed with 5 × loading buffer or non-reducing 5 × loading buffer and then heated at 37°C for 30 minutes. For

detection of glycosylation, protein samples were treated with PNGase F (Yeasen) or EndoH (New England Biolabs) according to the manufacturer's instructions. Using the Bio-Rad Trans-Blot System, proteins were transferred onto the NC membranes (10600002, Univ-bio) after being separated by SDS-polyacrylamide gel electrophoresis. Membranes were blocked for 1 hour at room temperature and incubated with primary antibody at 4°C overnight. For co-immunoprecipitation (Co-IP), one-tenth of the cell lysates were collected for input and the rest were rotated with anti-HA-magnetic beads (MCE) at room temperature for 2 hours. After 4 washes with lysis buffer, the samples were resuspended in loading buffer or non-reducing loading buffer and heated at 37°C for 30 minutes.

The following antibodies were used for immunoblots: rabbit anti-FLAG (20543-1-AP; Proteintech), goat anti-Norrin (AF3014; R&D Systems), rat anti-HA (3F10; Roche), rabbit anti-GAPDH (10494-1-AP; Proteintech), anti-rabbit, anti-goat, and anti-rat secondary antibody conjugated with horseradish peroxidase (SA0001-2, SA0001-4, and SA00001-15; Proteintech).

Immunofluorescence Staining

Cells grown on poly-l-lysine coated coverslips were washed with PBS twice and fixed with 4% PFA (Biosharp) at room temperature for 15 minutes. Coverslips were washed with PBS 3 times and then blocked with buffer (5% FBS and 0.2% Triton X-100 in PBS) for 30 minutes, and then incubated with primary antibodies diluted in blocking buffer for overnight at 4°C. On the next day, coverslips were washed with PBS 3 times and incubated with fluorescent secondary antibodies and DAPI (4083; CST) for 1 hour at room temperature. Fluorescence was visualized by LSM900 confocal microscope (Zeiss) using a 63 × oil objective. Co-localization analysis was performed using the Pearson correlation coefficient method in Fiji.

The following antibodies were used for immunofluorescence: rat anti-HA (3F10; Roche), mouse anti-FLAG (F1804; Sigma), chicken anti-GFP (A10262; ThermoFisher), rabbit anti-GM130 (52648; Abcam), Alexa fluor 488 donkey anti-chicken (A78948; ThermoFisher), Alexa fluor 633 goat anti-rat (A-21094; ThermoFisher), Alexa fluor 594 donkey anti-rabbit (R37119; ThermoFisher), and Alexa fluor 488 donkey anti-mouse (A-21202; ThermoFisher).

Dual-Luciferase Reporter Assay

For autocrine setting, HEK293STF cells were transfected with 175 ng DNA mix of 25 ng FZD4-HA, 25 ng LRP5, 100 ng pGL4.1-Renilla, and 25 ng *NDP* containing constructs in 24-well plates. After 48 hours, the transfected cells were subjected to luciferase activity assays using the Dual-Luciferase Reporter Assay System (Yeasen) according to the manufacturer's protocols. For paracrine setting, WT or mutant Norrin conditioned medium was adjusted to ensure consistent band intensity in Western blot analysis. Twenty-four hours after transfecting HEK293STF cells with a DNA mixture containing 25 ng FZD4-HA, 25 ng LRP5, and 100 ng pGL4.1-Renilla reporter genes in 24-well plates, the WT or mutant Norrin conditioned medium was added to the cells. Luciferase activity was measured after 24 hours. Relative activity was calculated as the ratio of firefly luciferase activity to Renilla luciferase activity. The presented values of each mutation were normalized against the WT.

Live-Cell Imaging Experiments and RUSH Assay

Live cells were imaged after transfection of indicated plasmids using an LSM900 confocal microscope (Zeiss) equipped with an incubation chamber with 5% CO_2 and a heated stage at 37°C. Images were acquired using a 63 × oil objective. RUSH assay was performed by treating HeLa or HEK293T cells transfected with WT RUSH construct or mutants in a complete medium containing 40 µM biotin (MCE).[25] Cells were then imaged for at least 2 hours or subjected to immunofluorescence staining after fixation with 4% PFA at the indicated time.

Statistical Analysis

Data were expressed as mean ± SD. One-way and 2-way analyses of variance (ANOVA) were used. All statistical evaluations and graphs were generated in GraphPad Prism version 8.0 software. Statistical significance was set at $P < 0.05$. $**P < 0.01$, $***P < 0.001$, and $****P < 0.0001$, and ns = not significant.

RESULTS

Mutations at the Norrin Dimer Interface Cause Defects in Norrin/β-Catenin Signaling

We conducted a comprehensive literature review, dating up until November 2023, encompassing reported missense mutations of the *NDP* gene in patients with FEVR and ND.[20,23,26–30] The mutations were categorized based on the functional domains they located in. Mutations occurring at the same location were counted as one. Among these mutations, 45.6% (26/57) were found to be located at the dimer interface, with their specific functional impact remaining unknown (Fig. 1A, Supplementary Table S2). To address this knowledge gap, our study delved into investigating the specific effects of 21 mutations within this dimer interface
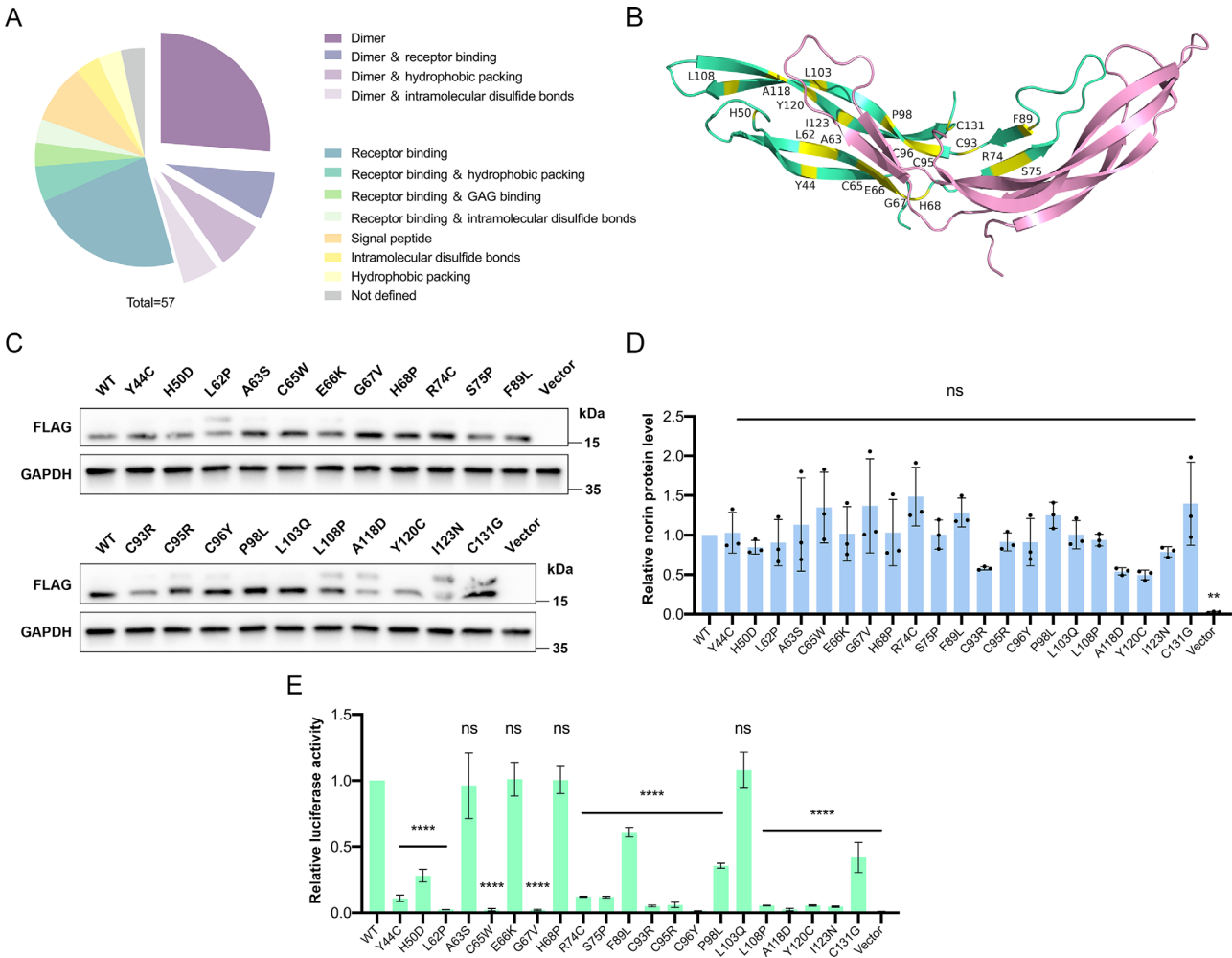

FIGURE 1. The expression level and Norrin/β-catenin signaling activity of mutations at the Norrin dimer interface. (**A**) Classification of Norrin functional domains and disease-associated mutations. (**B**) Crystal structure of the Norrin dimer using Pymol (PDB ID = 5BQB). Each monomer is colored *green* and *pink*. The mutations at the dimer interface studied in this research are colored in *yellow*. (**C**) Western blot of Myc-FLAG-tagged Norrin protein level in HEK293T cells transfected with WT, mutants, or vector plasmids ($n = 3$; Error bars, SD). (**D**) Densitometry analysis of Myc-FLAG-tagged Norrin protein level in HEK293T cells transfected with WT, mutants, or vector. (**E**) Relative luciferase activity in response WT, mutants, or vector plasmids in autocrine monoculture setting in the presence of FZD4/LRP5 ($n = 4$; Error bars, SD). One-way ANOVA with Dunnett's multiple comparisons test was performed to compare each mutant or vector and WT for (**D**) and (**E**). $**P < 0.01$; $****P < 0.0001$; ns, not significant.

TABLE. Dimer Interface Mutations Studied in this Research

Dimer Interface Mutation	Other Functional Domain Involved	Polyphen-2	PHRED-Like Scaled CADD Score	Reported Functional Analysis
Y44C	FZD4 binding, LGR4 binding	1.000/probably damaging	27.6	
H50D		0.999/probably damaging	27.2	
L62P		1.000/probably damaging	29.0	
A63S	FZD4 binding	0.958/probably damaging	23.8	
C65W	Intramolecular disulfide bonds	1.000/probably damaging	18.0	
E66K		1.000/probably damaging	24.3	
G67V		1.000/probably damaging	25.2	
H68P		0.001/benign	20.7	
R74C		1.000/probably damaging	27.3	
S75P		0.997/probably damaging	25.3	
F89L		0.999/probably damaging	24.3	
C93R		0.999/probably damaging	25.8	
C95R		0.999/probably damaging	29.5	
C96Y	Intramolecular disulfide bonds	0.999/probably damaging	27.4	
P98L		1.000/probably damaging	12.0	
L103Q	Hydrophobic packing	1.000/probably damaging	27.5	
L108P	Hydrophobic packing	1.000/probably damaging	27.9	Impaired Wnt signaling
A118D		0.994/probably damaging	29.3	
Y120C	FZD4 binding, hydrophobic packing	1.000/probably damaging	31.0	Impaired Wnt signaling
I123N	Hydrophobic packing	1.000/probably damaging	28.7	Impaired Wnt signaling
C131G		1.000/probably damaging	25.7	

In silico analyses used: PolyPhen-2 (http://genetics.bwh. harvard.edu/pph2/; provided in the public domain by Harvard University, Cambridge, MA, USA), PHRED- like Scaled CADD Score (https://cadd.gs.washington.edu/snv).

(Fig. 1B, see the Table). Because Norrin is a secreted protein, we tested a range of tags to enhance its secretion efficiency and facilitate detection. Ultimately, we selected a Norrin protein construct tagged with Myc-FLAG at the C-terminus for functional experiments due to its strong secretion capacity and robust activation of the Norrin/β-catenin signaling pathway (Supplementary Figs. S1A, S1B, S1C). It is worth noting that the introduction of the Myc tag led to a slightly larger band in Western blot detection of Norrin protein. We examined the Myc tag and Myc-FLAG tag at the C-terminus of the plasmid, as well as their NDP-linked sequences, and found that in the linker region, they both included the Asn-Ser-Thr sequence, which is the well-established Asn-linked glycosylation site (see Supplementary Table S1). Using deglycosylation enzymes,[31] we confirmed that this band corresponded to glycosylated Norrin (Supplementary Figs. S1D, S1E). We did not observe any significant impact of glycosylation on the subsequent experimental results. WT, mutant, and vector plasmids were expressed in HEK293T cells to assess the expression levels of Norrin protein in the cell lysates. All mutants showed expression levels similar to the WT (Figs. 1C, 1D). Subsequently, FZD4/LRP5 plasmids were co-transfected with Norrin (WT, mutant, or vector) into HEK293STF cells to evaluate the Norrin/β-catenin pathway activation ability of Norrin mutants under conditions of autocrine (Fig. 1E). It was found that apart from A63S, E66K, H68P, and L103Q, which displayed activation abilities similar to the WT, other mutations impaired their capacity to activate the Norrin/β-catenin pathway.

Proper Protein Assembly Is Associated With Secretion of Biological Active Norrin

To investigate how mutations affect Norrin/β-catenin pathway activation, considering that Norrin is a secreted protein, we first compared the level of Norrin protein in the cell culture medium. We found that most of the mutations resulted in a decrease in secretion efficiency, which was correlated with the extent of impairment in Norrin/β-catenin pathway activation (Figs. 2A, 2B). Furthermore, we subjected the collected medium to non-reducing SDS-PAGE to observe the difference in band size of secreted Norrin under non-reducing conditions (Figs. 2C, 2D). Sample loading was adjusted through denaturing and reducing SDS-PAGE to visualize the bands of each mutation. We observed 2 different bands, one with a molecular weight of about 65 KD and the other with a molecular weight of about 50 KD, for the WT and 4 mutants (A63S, E66K, H68P, and L103Q) that were unaffected in both Norrin/β-catenin pathway activation and secretion. H50D, F89L, P98L, and C131G retained some activation ability, with the first two showing bands of the same size, whereas the latter two did not. In contrast, other mutants displayed a remarkable smear pattern along with faster-migrating bands. The distinct bands exhibited under non-reducing conditions indicate abnormal protein dynamics of Norrin following dimer interface mutations, leading to inadequate oligomerization, impaired folding, or failure to form unknown protein complexes.

To determine whether the decrease in luciferase activity observed in mutants under autocrine settings was solely due to reduced secretion, we adjusted the collected supernatant loading volumes using denaturing and reducing SDS-PAGE and Western blot to ensure equal Norrin amounts. Twenty-four hours after transfection of FZD4/LRP5 in HEK293STF cells, an appropriate volume of WT or mutant Norrin supernatant was added to achieve uniform concentrations during incubation. Following 24 hours of incubation, measurement of luciferase activity consistently demonstrated impaired signaling pathway activation for the mutants, with differences in secretion efficiency being excluded as a contributing factor (Fig. 2E). To further verify the findings, we repeated the experiments in HeLa cells and the results were consistent with those obtained in HEK293T cells (Supple-
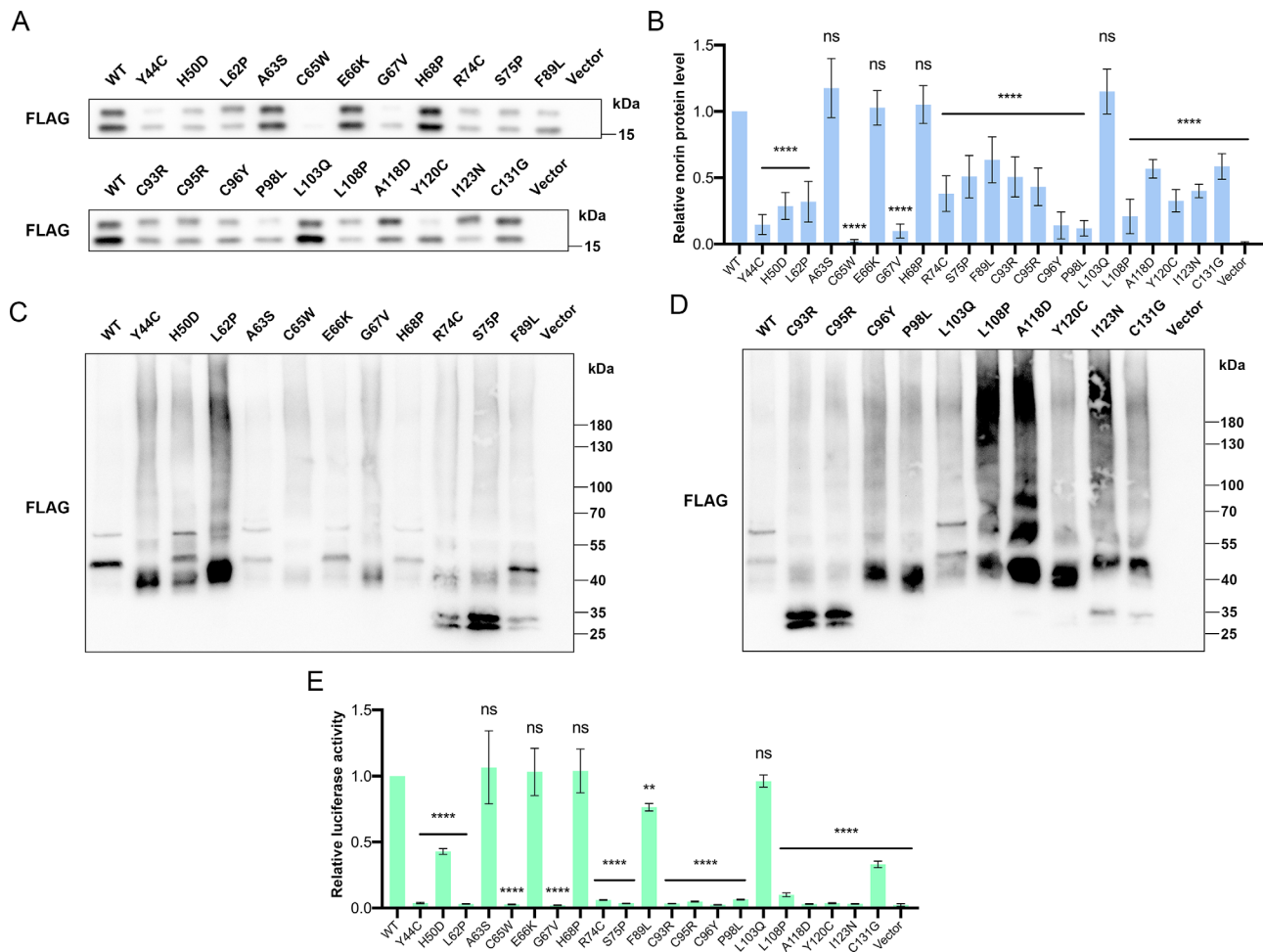
FIGURE 2. Mutations at the dimer interface affect secretion efficiency, protein assembly, and signaling activity of Norrin. Following the transfection of WT, mutant, or empty vector into HEK293T cells, the culture medium was collected after 48 hours. (**A**) Western blot of Myc-FLAG-tagged Norrin protein level in culture medium. (**B**) Densitometry analysis of Myc-FLAG-tagged Norrin protein level in culture medium ($n = 6$; Error bars, SD). (**C**) and (**D**) Under non-reducing conditions, Western blot analysis was performed to assess the protein assembly forms of Norrin in the culture medium. (**E**) Relative STF luciferase activity in response to the WT, mutants, or vector medium in the presence of FZD4/LRP5. It is worth noting that the medium contained equal amounts of norrin protein ($n = 4$; Error bars, SD). One-way ANOVA with Dunnett's multiple comparisons test was performed to compare each mutant or vector and WT for (**B**) and (**E**). ****$P < 0.0001$; ns, not significant.

mentary Figs. S2A, S2B). These results suggest that mutations in the dimeric interface of Norrin may lead to abnormal protein assembly, reduced secretion efficiency, and production of proteins with compromised biological activity.

Appropriate Protein Assembly Is Indispensable for the Binding of Norrin to FZD4 on the Cell Membrane

To further validate if the WT bands we observed in the non-reduced condition represent the active form, we performed Co-IP experiments in HEK293T cells by overexpressing norrin and FZD4-HA or FZD5-HA or vector. First, we verified that Norrin specifically interacts with FZD4, rather than FZD5 (Fig. 3A). Under non-reducing conditions, Norrin exhibited a smear pattern in the total cell lysate, which may represent various protein assembly states of Norrin during its production. However, when immunoprecipitated with FZD4, two bands of the same size as observed in

the medium were detected, suggesting that these bands could represent the state of FZD4-bound norrin on the cell membrane after secretion, which were supposed to be active forms of Norrin (Fig. 3B). Following this, in order to determine whether the mutated Norrin could bind to FZD4, we generated conditioned medium containing either the wild-type (WT) or mutated Norrin. After equalizing their quantities through Western blot, the conditioned media were used to incubate with HEK293T cells overexpressing FZD4 for Co-IP. Three mutants (C65W, C95R, and P98L), representing different amino acid interactions (hydrogen bonds, disulfide bridges, and hydrophobic interactions), were shown to compromise the interaction with FZD4 (Fig. 3C). Moreover, we used immunofluorescence staining to conduct co-localization analysis of Norrin and FZD4 in HeLa cells (Fig. 3D). It was found that the mutants with impaired Wnt activation ability lost their ability to co-localize with FZD4 on the membrane (Fig. 3E, Supplementary Fig. S3). Under live cell condition, it was also observed that the mutants failed to bind to membrane-localized FZD4 (Supplementary Fig. S4).

Figure 3. Dimer interface mutants are compromised in binding to FZD4. (**A**) and (**B**) Western blot analysis of NDP-Myc-FLAG co-immunoprecipitated with FZD4-HA, FZD5-HA, or vector. (**A**) Under reducing condition. (**B**) Under non reducing condition. (**C**) Western blot analysis of Norrin conditioned medium (WT or mutants) co-immunoprecipitated with FZD4-HA. (**D**) Representative immunofluorescence images of NDP (*green*), FZD4 (*magenta*), and DAPI (*blue*) in HeLa cells transfected with NDP-Myc-FLAG (WT or mutants) and FZD4-HA (Scale bars = 5 μm). The relative fluorescence intensity plot on the right was generated by the Zen software. It shows the fluorescence intensity values of the two channels along the *white line*, with the highest fluorescence intensity value normalized to 100%. (**E**) Quantification results are shown as mean ± SD obtained from 3 independent experiments, with 50 cells analyzed in each experiment. One-way ANOVA with Dunnett's multiple comparisons test was performed to compare each mutant and WT for (**E**). ****$P < 0.0001$; ns, not significant.
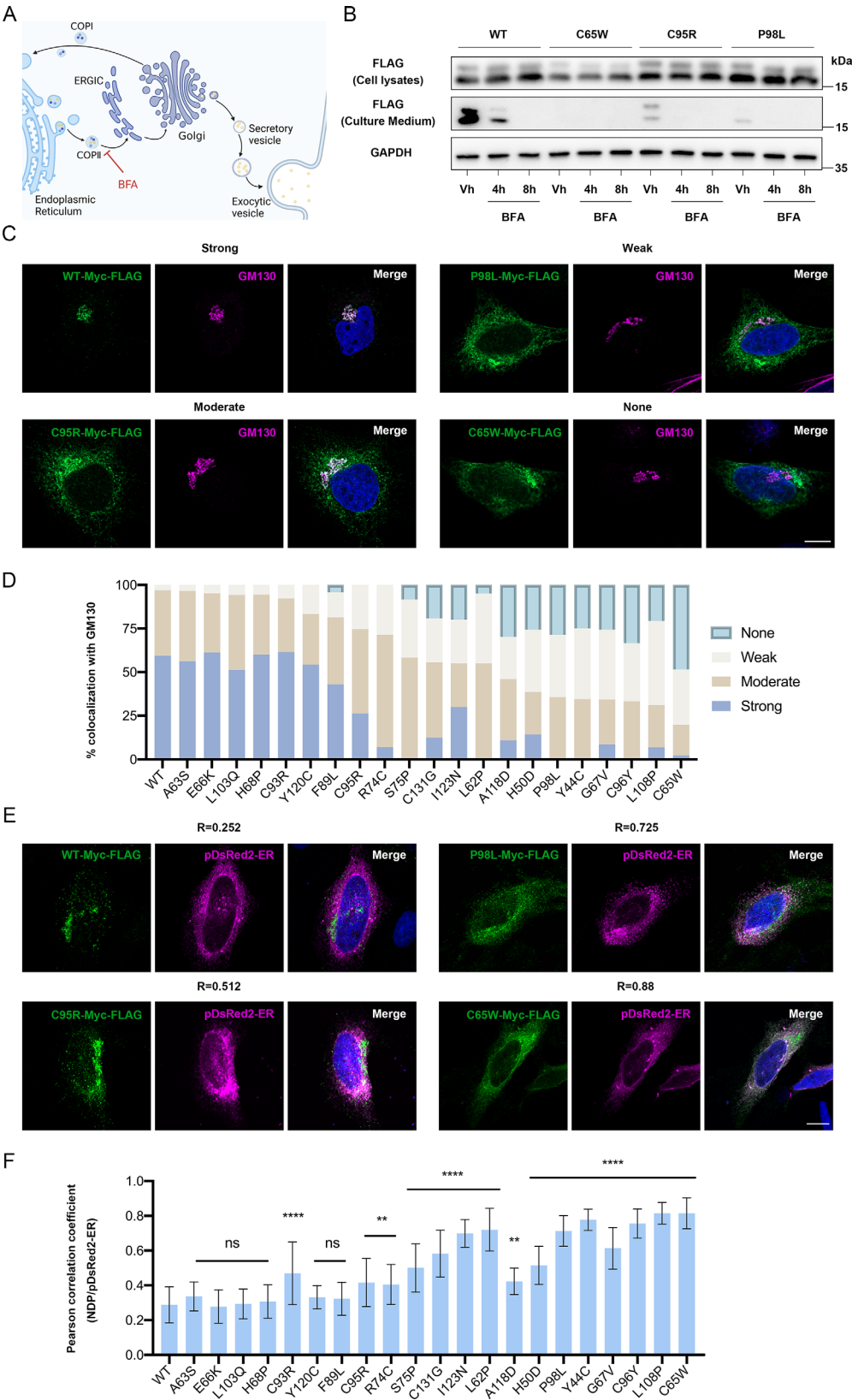
Figure 4. Mutations at the dimer interface impair secretion efficiency and subcellular localization of Norrin. (**A**) Schematic representation of conventional secretory pathway. (**B**) Western blot analysis of NDP-Myc-FLAG (WT or mutants) in cell lysates and culture medium in the presence of BFA. Vh = vehicle. (**C**) Representative immunofluorescence images of NDP (*green*), GM130 (*magenta*), and DAPI (*blue*) in HeLa cells transfected with NDP-Myc-FLAG (WT or mutants; Scale bar = 10 μm). "Strong" representing a significant accumulation of Norrin within the Golgi apparatus. "Moderate" indicating a notable localization of Norrin in the Golgi apparatus. "Weak" indicating no apparent Golgi apparatus accumulation but some degree of co-localization. "None" representing absence of co-localization between Norrin and the

Golgi apparatus. (**D**) The graph shows the percentage of different colocalization state with GM130. More than 50 cells are counted per condition. (**E**) Representative immunofluorescence images of NDP (*green*), ER (*magenta*), and DAPI (*blue*) in HeLa cells transfected with NDP-Myc-FLAG (WT or mutants) and pDsRed2-ER (Scale bar = 10 µm). (**F**) Co-localization was quantified using the Pearson correlation coefficient ($n = 20$; Error bars, SD). One-way ANOVA with Dunnett's multiple comparisons test was performed to compare each mutant and WT for (**F**). **$P < 0.01$; ****$P < 0.0001$; ns, not significant.

These results indicate the necessity of proper protein assembly for Norrin to bind to FZD4.

Secretion-Defective Mutant Proteins Are Retained in the ER

Mutations at the dimer interface not only weaken its activation ability but also lead to a decrease in secretion efficiency of Norrin. Prior to this study, there was no literature investigating the secretion of Norrin. Because the amino acid sequence of Norrin contains a signal peptide at the N-terminus (amino acids 1–24), we hypothesized that it may be secreted via the conventional secretory pathway.[32] The conventional secretory pathway is a cellular process that transports newly synthesized proteins from the ER to their final destinations through the Golgi apparatus, involving vesicular transport and protein modification (Fig. 4A).[33] We treated cells with Brefeldin A (BFA) to block ER exit of proteins and examined whether the secretion of Norrin into the supernatant was reduced (Fig. 4B).[34] Indeed, after BFA treatment, both WT and mutant Norrin showed a significant decrease in the supernatant and an increase in the cell lysates. Furthermore, we investigated the co-localization relationship between WT or mutant norrin and the Golgi apparatus in an overexpression setting. HeLa cells were transfected with WT or mutant plasmids, followed by analysis of the co-localization with the cis-Golgi marker GM130.[35] We classified the co-localization of Norrin with the Golgi apparatus into four categories (Fig. 4C). WT Norrin and mutants unaffected in secretion displayed mainly strong and moderate co-localization with the Golgi apparatus, whereas mutants with reduced secretion efficiency showed compromised co-localization (Fig. 4D). Additionally, analysis of co-localization with the ER revealed that mutants with reduced secretion efficiency were more likely to co-localize with the ER rather than the Golgi, which was further confirmed under live cell condition (Figs. 4E, 4F, Supplementary Fig. S5). The above results indicate that Norrin is secreted via the conventional secretory pathway, and mutations at the dimer interface of Norrin can affect its subcellular localization, leading to impaired Golgi apparatus localization and increased co-localization with the ER. This disruption in proper protein trafficking contributes to the reduced secretion efficiency observed in these mutant forms of Norrin.

Visualization and Characterization of Norrin Secretion Dynamics Using the RUSH Assay

The previous immunofluorescence results provided insights into the subcellular localization of Norrin during overexpression. However, they were unable to capture the dynamic secretion process of Norrin. In order to address this limitation, we utilized the RUSH system to visually monitor the exit of Norrin from the ER.[25] In the RUSH assay, HeLa cells were transfected with plasmids containing *NDP* fused downstream of streptavidin binding peptide (SBP) and EYFP. This plasmid also encodes streptavidin fused to an isoform of Ii

containing an N-terminal arginine-based motif, which retains it in the ER. The binding between streptavidin and SBP leads to the retention of NDP-SBP-EYFP in the ER. However, when cells are treated with biotin, SBP is released from streptavidin, causing the release of NDP-SBP-EYFP from the ER (Figs. 5A, 5B, 5F, Supplementary Video S1).

After a 25-minute biotin incubation, more than 80% of the cells transfected with the WT RUSH construct exhibited an accumulation of fluorescence in the juxta-nuclear region, which was subsequently confirmed to be the Golgi apparatus (Figs. 5C, 5G). In contrast, C95R and P98L showed a significant delay in their appearance in the Golgi apparatus, whereas C65W hardly localized to the Golgi apparatus (Fig. 5D). After accumulating in the Golgi apparatus, WT Norrin was completely released via vesicles approximately 35 minutes later, with no visible Golgi-like fluorescence accumulation remaining in the cells. In comparison, the exit of C95R and P98L from the Golgi apparatus was significantly delayed (Fig. 5E). The degree of delay in both ER and Golgi exit was positively correlated with the reduction in secretion efficiency. We repeated these experiments in HEK293T cells and obtained similar results (Supplementary Fig. S6). The RUSH assay provided further validation for the observed secretion deficiency in mutants. This deficiency was attributed to their impaired ability to effectively exit the ER and access the Golgi apparatus, as well as their compromised vesicle-mediated transport during departure from the Golgi apparatus.

Discussion

In this study, we explored the effects of 21 *NDP* mutations located at the dimer interface, which have been rarely investigated before. Of note, among these mutations, four (A63S, E66K, H68P, and L103Q) exhibited similar properties to the WT in terms of protein assembly, secretion efficiency, and activation of the Norrin/β-catenin signaling pathway. Thus, we posit that Norrin may possess additional functions that have yet to be discovered, and the results of our in vitro overexpression experiments may not fully reflect the in vivo situation. In addition to this, we did not perform the assay in Müller glial cells that normally secrete Norrin in the eye, nor in vascular endothelial cells, which are important target cells for Norrin in the retina.[24] Further studies are needed to understand the pathogenic mechanisms of these mutations in patients. In contrast, the other 17 mutations showed impaired activation of the Wnt signaling pathway. The investigation of these mutations unveiled an aberrant protein assembly pattern in the culture medium, along with a reduced ability to bind to FZD4 on the cell membrane. Co-IP experiments with FZD4 revealed that under non-reducing condition, the sizes of WT Norrin bands in the medium were consistent with those bound to FZD4. Mutations that failed to generate the correct form were associated with decreased FZD4 binding. Mutations with milder impairment in activation, such as H50D and F89L, exhibited bands partially resembling the WT in the medium and retained some FZD4
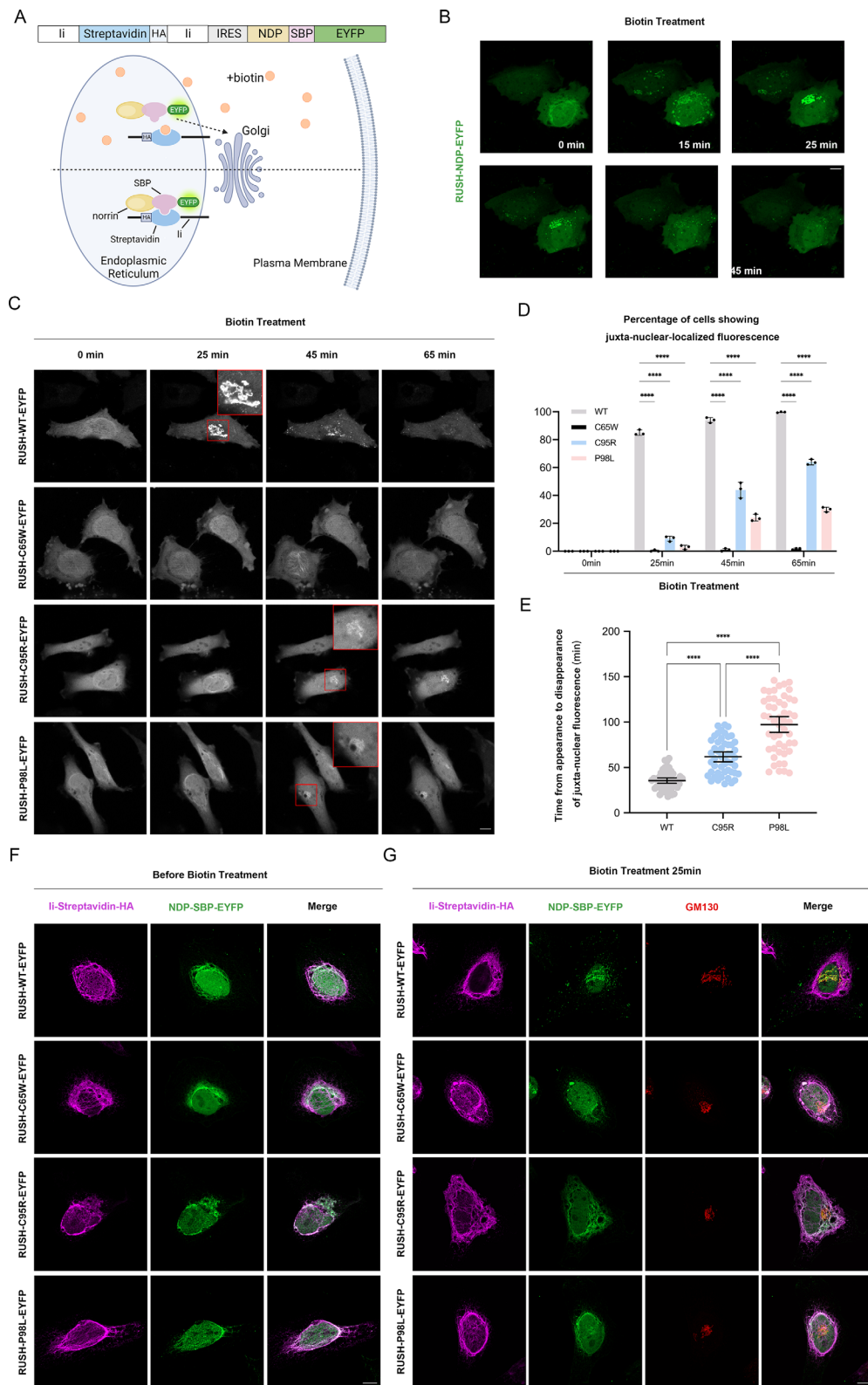
FIGURE 5. Synchronization of norrin secretion using the RUSH system. (**A**) Schematic of the RUSH plasmid construct and system. Under physiological conditions, Ii-streptavidin-HA binds to NDP-SBP-EYFP to retain the protein in the ER. After addition of 40 µM biotin, NDP-SBP-EYFP is released and transported to the Golgi and subsequently to the plasma membrane. (**B**) Fluorescence images of HeLa cells expressing RUSH-NDP-EYFP at various time points after biotin addition (from Supplementary Video S1). At time 00:00 (minutes:seconds) of biotin addition, norrin remained in the ER. At time 15:00, Norrin starts to leave the ER and can be seen in the juxtanuclear region. At around time 25:00, Norrin is seen entirely in the juxtanuclear region. Starting around 35:00 Norrin can be seen in vesicle exiting the juxtanuclear region and moving toward the periphery. By time 65:00, the juxtanuclear region appears to be depleted of Norrin. (**C**) HeLa cells were transfected with RUSH plasmids encoding WT Norrin or mutants. The localization of the different versions of RUSH constructs was analyzed

after incubation with biotin for the indicated time. The highlighted and magnified area in the *red box* indicates the presence of Norrin in the juxtanuclear region (Scale bar = 10 μm). (**D**) Quantifications of the percentage of cells showing juxta-nuclear–accumulated EYFP signal after incubation with biotin for the indicated time (mean ± SD; $n = 3$; >50 cells counted for each time point). (**E**) Quantification of the time from the appearance to the disappearance of the juxta-nuclear region EYFP signal, mean ± SD; $n = 50$ cells counted for each condition. (**F**) Representative immunofluorescence images of Ii-streptavidin-HA (anti-HA, *magenta*), NDP-SBP-EYFP (anti-GFP, *green*) in HeLa cells transfected with RUSH constructs (WT or mutants) before incubation with biotin (Scale bar = 10 μm). (**G**) Representative immunofluorescence images of Ii-streptavidin-HA (anti-HA, *magenta*), NDP-SBP-EYFP (anti-GFP, *green*) and GM130 (anti-GM130, *red*) in HeLa cells transfected with RUSH constructs (WT or mutants) after incubation with biotin for 25 minutes (Scale bar = 10 μm). Two-way ANOVA with Dunnett's multiple comparisons test was performed to compare each mutant and WT at the indicated time for (**D**). One-way ANOVA with Tukey's multiple comparisons test was performed to compare each construct at the indicated time for (**E**). ****$P < 0.0001$

binding ability. The ability to bind to FZD4 corresponded to the mutants' capacity to activate the Wnt signaling pathway. These results confirm the necessity of proper Norrin protein assembly for FZD4 binding.

Among the 21 mutations studied, reduced secretion in the medium was observed in 17 mutations. For the first time, we demonstrated Norrin secretion via the conventional secretory pathway and found that overexpressed WT Norrin mainly localized to the Golgi apparatus in HeLa cells, whereas mutations with reduced secretion exhibited decreased co-localization with the Golgi apparatus and increased localization to the ER. The severity of mislocalization correlated with the extent of reduced secretion. Using the RUSH assay, we observed the dynamic process of Norrin exiting the ER, reaching the Golgi apparatus, and subsequently being released from the Golgi via vesicles. The mutant C65W, with the lowest secretion levels, almost failed to reach the Golgi apparatus, whereas C95R and P98L exhibited significant delays compared to the WT in both ER exit and Golgi release. Based on these findings, we propose that the proper protein assembly form of Norrin plays a role in mediating protein-protein interactions necessary for proper trafficking. Mutations at the dimer interface may disrupt these interactions, affecting the recruitment of chaperones or cargo receptors. Further research is warranted to identify specific chaperones or cargo receptors involved in Norrin trafficking. Although this study examined nearly all Norrin mutations at the dimer interface, the question of whether mutations in other domains can also result in secretion impairment requires future investigation.

We believe the process of Norrin secretion is an underexplored area of cellular research. Previous reports have suggested that Norrin may function as a modulator of human brain cancer progression and be involved in the astroglial regulation of neuronal function in the cortex[36,37]. Exploring the regulatory proteins involved in Norrin secretion and investigating the presence of modifications in Norrin represents an intriguing direction for further research. Additionally, modulating Norrin secretion may hold potential as a therapeutic strategy for brain disorders characterized by dysregulated astroglial function. Although research in this area is still in its early stages, targeting Norrin secretion may offer novel avenues for meaningful clinical interventions.

Disclosure: **M. Liu**, None; **E. Dai**, None; **M. Yang**, None; **S. Li**, None; **L. Fan**, None; **Y. Liu**, None; **H. Xiao**, None; **P. Zhao**, None; **Z. Yang**, None

References

1. Wang Z, Liu CH, Huang S, Chen J. Wnt signaling in vascular eye diseases. *Prog Retin Eye Res.* 2019;70:110–133.
2. Khan K, Logan CV, McKibbin M, et al. Next generation sequencing identifies mutations in Atonal homolog 7 (ATOH7) in families with global eye developmental defects. *Hum Mol Genet.* 2012;21:776–783.
3. Downey LM, Keen TJ, Roberts E, Mansfield DC, Bamashmus M, Inglehearn CF. A new locus for autosomal dominant familial exudative vitreoretinopathy maps to chromosome 11p12-13. *Am J Hum Genet.* 2001;68:778–781.
4. Park H, Yamamoto H, Mohn L, et al. Integrin-linked kinase controls retinal angiogenesis and is linked to Wnt signaling and exudative vitreoretinopathy. *Nat Commun.* 2019;10:5243.
5. Jiao X, Ventruto V, Trese MT, Shastry BS, Hejtmancik JF. Autosomal recessive familial exudative vitreoretinopathy is associated with mutations in LRP5. *Am J Hum Genet.* 2004;75:878–884.
6. Li S, Yang M, He Y, et al. Variants in the Wnt co-receptor LRP6 are associated with familial exudative vitreoretinopathy. *J Genet Genomics.* 2022;49:590–594.
7. Toomes C, Bottomley HM, Jackson RM, et al. Mutations in LRP5 or FZD4 underlie the common familial exudative vitreoretinopathy locus on chromosome 11q. *Am J Hum Genet.* 2004;74:721–730.
8. Junge HJ, Yang S, Burton JB, et al. TSPAN12 regulates retinal vascular development by promoting Norrin- but not Wnt-induced FZD4/beta-catenin signaling. *Cell.* 2009;139:299–311.
9. Chen ZY, Battinelli EM, Fielder A, et al. A mutation in the Norrie disease gene (NDP) associated with X-linked familial exudative vitreoretinopathy. *Nat Genet.* 1993;5:180–183.
10. Collin RW, Nikopoulos K, Dona M, et al. ZNF408 is mutated in familial exudative vitreoretinopathy and is crucial for the development of zebrafish retinal vasculature. *Proc Natl Acad Sci USA.* 2013;110:9856–9861.
11. Mears K, Bakall B, Harney LA, Penticoff JA, Stone EM. Autosomal dominant microcephaly associated with congenital lymphedema and chorioretinopathy due to a novel mutation in KIF11. *JAMA Ophthalmol.* 2015;133:720–721.
12. Zhu X, Yang M, Zhao P, et al. Catenin alpha 1 mutations cause familial exudative vitreoretinopathy by overactivating Norrin/beta-catenin signaling. *J Clin Invest.* 2021;131:e139869.
13. Dixon MW, Stem MS, Schuette JL, Keegan CE, Besirli CG. CTNNB1 mutation associated with familial exudative vitreoretinopathy (FEVR) phenotype. *Ophthalmic Genet.* 2016;37:468–470.

14. Zhang L, Zhang X, Xu H, et al. Exome sequencing revealed Notch ligand JAG1 as a novel candidate gene for familial exudative vitreoretinopathy. *Genet Med*. 2020;22:77–84.

15. Zhang S, Li X, Liu W, et al. Whole-exome sequencing identified DLG1 as a candidate gene for familial exudative vitreoretinopathy. *Genet Test Mol Biomarkers*. 2021;25:309–316.

16. Yang M, Li S, Huang L, et al. CTNND1 variants cause familial exudative vitreoretinopathy through the Wnt/cadherin axis. *JCI Insight*. 2022;7:e158428.

17. Xu N, Cai Y, Li J, et al. An SNX31 variant underlies dominant familial exudative vitreoretinopathy-like pathogenesis. *JCI Insight*. 2023;8:e167032.

18. Li S, Yang M, Zhao R, et al. Defective EMC1 drives abnormal retinal angiogenesis via Wnt/beta-catenin signaling and may be associated with the pathogenesis of familial exudative vitreoretinopathy. *Genes Dis*. 2023;10:2572–2585.

19. Ohlmann A, Tamm ER. Norrin: molecular and functional properties of an angiogenic and neuroprotective growth factor. *Prog Retin Eye Res*. 2012;31:243–257.

20. Wawrzynski J, Patel A, Badran A, Dowell I, Henderson R, Sowden JC. Spectrum of mutations in NDP resulting in ocular disease; a systematic review. *Front Genet*. 2022;13:884722.

21. Kondo H. Complex genetics of familial exudative vitreoretinopathy and related pediatric retinal detachments. *Taiwan J Ophthalmol*. 2015;5:56–62.

22. Xu Q, Wang Y, Dabdoub A, et al. Vascular development in the retina and inner ear: control by Norrin and Frizzled-4, a high-affinity ligand-receptor pair. *Cell*. 2004;116:883–895.

23. Chang TH, Hsieh FL, Zebisch M, Harlos K, Elegheert J, Jones EY. Structure and functional properties of Norrin mimic Wnt for signalling with Frizzled4, Lrp5/6, and proteoglycan. *Elife*. 2015;4:e06554.

24. Wang Y, Rattner A, Zhou Y, Williams J, Smallwood PM, Nathans J. Norrin/Frizzled4 signaling in retinal vascular development and blood brain barrier plasticity. *Cell*. 2012;151:1332–1344.

25. Boncompain G, Divoux S, Gareil N, et al. Synchronization of secretory protein traffic in populations of cells. *Nat Methods*. 2012;9:493–498.

26. Kondo H, Qin M, Kusaka S, et al. Novel mutations in Norrie disease gene in Japanese patients with Norrie disease and familial exudative vitreoretinopathy. *Invest Ophthalmol Vis Sci*. 2007;48:1276–1282.

27. Ke J, Harikumar KG, Erice C, et al. Structure and function of Norrin in assembly and activation of a Frizzled 4-Lrp5/6 complex. *Genes Dev*. 2013;27:2305–2319.

28. Musada GR, Jalali S, Hussain A, et al. Mutation spectrum of the Norrie disease pseudoglioma (NDP) gene in Indian patients with FEVR. *Mol Vis*. 2016;22:491–502.

29. Tang M, Sun L, Hu A, et al. Mutation spectrum of the LRP5, NDP, and TSPAN12 genes in Chinese patients with familial exudative vitreoretinopathy. *Invest Ophthalmol Vis Sci*. 2017;58:5949–5957.

30. Li JK, Li Y, Zhang X, et al. Spectrum of variants in 389 Chinese probands with familial exudative vitreoretinopathy. *Invest Ophthalmol Vis Sci*. 2018;59:5368–5381.

31. Schjoldager KT, Narimatsu Y, Joshi HJ, Clausen H. Global view of human protein glycosylation pathways and functions. *Nat Rev Mol Cell Biol*. 2020;21:729–749.

32. Walter P, Gilmore R, Blobel G. Protein translocation across the endoplasmic reticulum. *Cell*. 1984;38:5–8.

33. Viotti C. ER to Golgi-dependent protein secretion: the conventional pathway. *Methods Mol Biol*. 2016;1459:3–29.

34. Grose C, Klionsky DJ. Alternative autophagy, brefeldin A and viral trafficking pathways. *Autophagy*. 2016;12:1429–1430.

35. Nakamura N, Rabouille C, Watson R, et al. Characterization of a cis-Golgi matrix protein, GM130. *J Cell Biol*. 1995;131:1715–1726.

36. El-Sehemy A, Selvadurai H, Ortin-Martinez A, et al. Norrin mediates tumor-promoting and -suppressive effects in glioblastoma via Notch and Wnt. *J Clin Invest*. 2020;130:3069–3086.

37. Miller SJ, Philips T, Kim N, et al. Molecularly defined cortical astroglia subpopulation modulates neurons via secretion of Norrin. *Nat Neurosci*. 2019;22:741–752.